01-8; methyl phenanthrene-9-carboxylate/ethyl dichloroaluminum complex, 139871-24-2; phenanthrene-9-carboxamide/boron trifluoride complex, 139871-25-3; *N*-methylphenanthrene-9-carboxamide/boron trifluoride complex, 139871-26-4; *N,N*-dimethylphenanthrene-9-carboxamide/boron trifluoride complex, 139871-27-5; phenanthrene-9-carboxamide/boron trichloride complex, 139871-28-6; phenanthrene-9-carboxamide/boron tribromide complex, 139871-29-7; *N,N*-dimethylphenanthrene-9-carboxamide/boron tribromide complex, 139871-30-0.

A Study of Norrish Type II Reactions of Aryl Alkyl Ketones Included within Zeolites

V. Ramamurthy,*,† D. R. Corbin,† and L. J. Johnston*,‡

Contribution from Central Research and Development, Experimental Station, The Du Pont Company,§ Wilmington, Delaware 19880-0328, and Steacie Institute for Molecular Sciences, National Research Council of Canada,∥ Ottawa, Ontario K1A 0R6, Canada.
Received September 27, 1991. Revised Manuscript Received January 10, 1992

Abstract: The photochemical and photophysical behavior of a large number of phenyl alkanones included in zeolites has been investigated. The interior size and shape of the zeolites control the behavior of the triplet ketone as well as that of the 1,4-diradical generated by Norrish type II γ-hydrogen abstraction. A relationship between the size and shape of the reaction cavity and the extent of the restrictions on the triplet ketone and the diradical intermediate has been observed. A model based on the "reaction cavity" concept has been valuable in understanding the unique influence of the zeolite on the reaction course of the type II process.

Introduction

The Norrish type II reaction is a mechanistically well understood reaction and has been extensively studied in both isotropic[1] and anisotropic media.[2] The efficiency of product formation from the excited triplet state via type II hydrogen abstraction, the ratio of elimination to cyclization products, and the ratio of *cis*- to *trans*-cyclobutanols from the type II 1,4-diradical are sensitive to the environment. We envisioned that a study of the Norrish type II reactions of aryl alkyl ketones within various zeolites would yield information concerning the restriction provided by the internal structure of the zeolite on the reaction course. This, in conjunction with further studies for these and other systems, would aid in the long-range prediction of the photophysical and photochemical behavior of guest molecules included within zeolites.[3] In this context, we have utilized a large number of zeolites as hosts to carry out phototransformations of several aryl alkyl ketones (Scheme I). A comprehensive photochemical investigation of **1** has also been conducted within faujasite zeolites (X and Y). This includes alteration of the characteristics of the cage by cation exchange (Li, Na, K, Rb, and Cs) and by inclusion of a cohost such as solvent hexane. The dramatic difference in product distribution observed between faujasite and pentasil zeolites as hosts led us to undertake a flash photolysis investigation of valerophenone in these zeolites. Results of such studies, as well as those from a steady-state photophysical investigation, are presented herein.

Zeolites may be regarded as open structures of silica in which aluminum has been substituted in a fraction of the tetrahedral sites.[4] The frameworks thus obtained contain pores, channels, and cages. The substitution of trivalent aluminum ions for a fraction of the tetravalent silicon ions at lattice positions results in a network that bears a net negative charge, which must be compensated by other counterions. The latter are mobile and may occupy various exchange sites depending on their radius, charge, and degree of hydration. They can be replaced, to varying degrees, by exchange with other cations. If zeolite water is removed, many other organic and inorganic molecules can be accommodated in the intracrystalline cavities.

A brief description of the structure of the zeolites used in this study is appropriate.[4] The topological structure of X- and Y-type zeolites consists of an interconnected three-dimensional network of relatively large spherical cavities, termed supercages (diameter of about 13 Å, Figure 1). Each supercage is connected tetrahedrally to four other supercages through 8-Å windows or pores. The interiors of zeolites X and Y also contain, in addition to supercages, smaller sodalite cages. The windows to the sodalite cages are too small to allow organic molecules access to these cages. Charge-compensating cations present in the internal structure are known to occupy three different positions (Figure 1) in zeolites X and Y. Only cations of sites II and III are expected to be readily accessible to the adsorbed organic molecule.

Among the medium-pore-sized zeolites, perhaps the most studied are the pentasil zeolites, ZSM-5 and ZSM-11 (Figure 1). These zeolites also have three-dimensional pore structures; a major difference between the pentasil pore structures and the faujasites described above is the fact that the pentasil pores do not link cage structures as such. Instead, the pentasils are composed of two intersecting channel systems. For ZSM-5, one system consists of straight channels with a free diameter of about 5.4 × 5.6 Å and the other consists of sinusoidal channels with a free diameter

† The Du Pont Company.
‡ National Research Council of Canada.
§ Contribution No. 5994.
∥ NRCC No. 33262.

(1) Wagner, P. J.; Park, B. S. *Org. Photochem.* **1991**, *11*, 227. Wagner, P. J. *Acc. Chem. Res.* **1971**, *4*, 168. Turro, N. J.; Dalton, J. C.; Dawes, K.; Farrington, G.; Hautala, R.; Morton, D.; Niemczyk, M.; Schore, N. *Acc. Chem. Res.* **1972**, *5*, 92. Scaiano, J. C. *Acc. Chem. Res.* **1982**, *15*, 252.
(2) Weiss, R. G. *Tetrahedron* **1988**, *44*, 3413. Scheffer, J. R. In *Organic Solid State Chemistry*; Desiraju, G., Ed.; Elsevier: Amsterdam, 1987; p 1. Ramamurthy, V.; Eaton, D. F. *Acc. Chem. Res.* **1988**, *21*, 300.
(3) Turro, N. J.; Garcia-Garibay, M. In *Photochemistry in Organized and Constrained Media*; Ramamurthy, V., Ed.; VCH: New York, 1991; p 1. Ramamurthy, V. In *Photochemistry in Organized and Constrained Media*; Ramamurthy, V., Ed.; VCH: New York, 1991; p 429.
(4) Meier, W. M.; Olson, D. H. *Atlas of Zeolite Structure Types*, 2nd revised ed.; Butterworths: Cambridge, 1987. Breck, D. W. *Zeolite Molecular Sieves: Structure, Chemistry, and Use*; John Wiley and Sons: New York, 1974. Dyer, A. *An Introduction to Zeolite Molecular Sieves*; John Wiley and Sons: Bath, 1988. van Bekkum, H., Flanigen, E. M., Jansen, J. C., Eds. *Introduction to Zeolite Science and Practice*; Elsevier: Amsterdam, 1991.

0002-7863/92/1514-3870$03.00/0

Scheme I

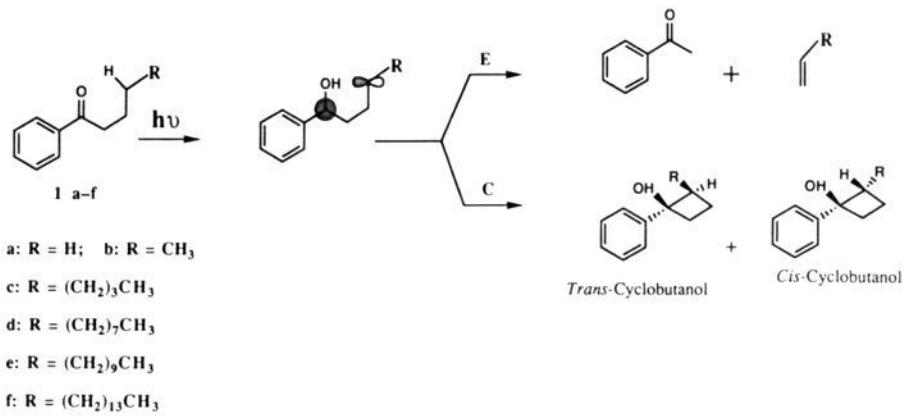

Table I. Size of Pore Openings and Dimensionality of the Pore System for Selected Medium-Pore and Large-Pore Molecular Sieves[a]

molecular sieve name	pore (window) size (Å)	channel or cage size
faujasite (X and Y type)	7.4	three-dimensional channel with a cage ($d \sim 12$ Å)
Ω	7.5 (3.4 × 5.6)	two non-interconnected channels
Linde type L	7.1	single channel with a lobe ($d \sim 7.5$ Å)
mordenite	7.0 × 6.7 and (2.6 × 5.7)	two interconnected channels
offretite	6.7 and (3.6 × 4.9)	two interconnected channels
ZSM-34	6.7 and (3.6 × 4.9)	two interconnected channels
ZSM-11	5.3 × 5.4	two interconnected channels
ZSM-5	5.3 × 5.6 and 5.1 × 5.5	two interconnected channels
θ-1	4.4 × 5.5	single channel
4A	4.2	three-dimensional channel with a cage ($d \sim 12$ Å)

[a] Meier, W. M.; Olson, D. H. In *Atlas of Zeolite Structure Types*, 2nd revised ed.; Butterworths: Cambridge, 1987. Breck, D. W. *Zeolite Molecular Sieves: Structure, Chemistry, and Use*; John Wiley and Sons: New York, 1974.

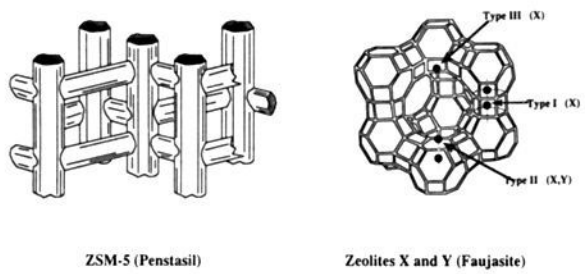

Figure 1. Structures of zeolites: faujasites and ZSM-5.

of about 5.1 × 5.5 Å. For ZSM-11, both are straight channels with dimensions of about 5.3 × 5.4 Å. The volume at the intersections of these channels is estimated to be 370 Å^3 for a free diameter of about 8.9 Å. Other zeolites of interest for photochemical studies include the LZ-L, mordenite, offretite, Ω, and β (Table I).

Several studies that are directly relevant to our work have been reported. Turro and Wan[5] have demonstrated in a preliminary study that the type II product distribution, upon photolysis of valerophenone and octanophenone, depends on the nature of the zeolite (Na X, Na Y, Na M-5, or silicalite) in which they are included. Casal and Scaiano[6a] have investigated the luminescent properties of valerophenone and β-arylpropiophenones included in silicalite (which has a structure identical to that of ZSM-5). While phosphorescence was observed from the latter at room temperature, the former did not exhibit phosphorescence. A time-resolved diffuse reflectance study of triplet butyrophenone and valerophenone included in silicalite has also been conducted by Wilkinson et al.[6b] The above studies serve as a basis for our comprehensive investigation of the type II reaction of aryl alkyl ketones included in a number of zeolites.[6c]

(5) Turro, N. J.; Wan, P. *Tetrahedron Lett.* **1984**, *25*, 3655.
(6) (a) Casal, H. L.; Scaiano, J. C. *Can. J. Chem.* **1985**, *63*, 1308. (b) Wilkinson, F.; Willsher, C. J.; Casal, H.; Johnston, L.; Scaiano, J. C. *Can. J. Chem.* **1986**, *64*, 539. (c) Ramamurthy, V.; Corbin, D. R.; Eaton, D. F. *J. Chem. Soc., Chem. Commun.* **1989**, 1213.

Results

General Sample Preparation and Photolysis. Zeolites stored under laboratory conditions are hydrated, and the supercages are filled with water. In general, these fail to include organic molecules from either solution or the vapor phase. Therefore, water must be removed from the cages by activating the zeolite at 500 °C for about 12 h in an aerated medium. The loss of water from the interior of the zeolite is not accompanied by any other structural changes. Such activated zeolites are used as the "hosts" in the present study. Nonpolar solvents such as hexane, pentane, and cyclohexane were found to be the best solvents for incorporation of the ketones into the zeolites. The low affinity of ketones for nonpolar solvents and of the solvent for the zeolite interior results in the efficient distribution of ketones **1a–f** within the zeolite.

Samples for which ketones **1a–f** were adsorbed onto the internal microporous structure of the zeolites were used for all of our photolyses and photophysical studies. Most of these studies were conducted on solvent-free, dry, solid samples. In all cases, the loading level was kept low and corresponded to an occupancy number (number of guest molecules/number of available supercages, $\langle S \rangle$) of about 0.2 for the X and Y zeolites. Complexes were prepared by stirring activated zeolites with appropriate amounts of ketone in hexane. The solvent was removed by filtration, and the complexes were washed with hexane and dried by degassing of the samples at low pressures (10^{-5} mm) for several hours. Further handling of the samples was done under laboratory conditions, and no special precautions were taken.

Generally, the photolysis products (2 h, <15% conversion as compared to a similar conversion in about 15 min in benzene) were extracted with ether. In each case, one experiment was conducted in which the products were isolated by dissolving the zeolite framework with concentrated HCl followed by extraction with ether. Product distributions obtained by these two methods (ether extractions with and without acid) were identical within 5%. Material balance in general was ~90%. These protocols ensured that no unidentified products were trapped within the zeolite framework. Products were analyzed by gas chromatography. For comparison, the ketones were also irradiated in benzene, hexane, and methanol in the absence of zeolite.

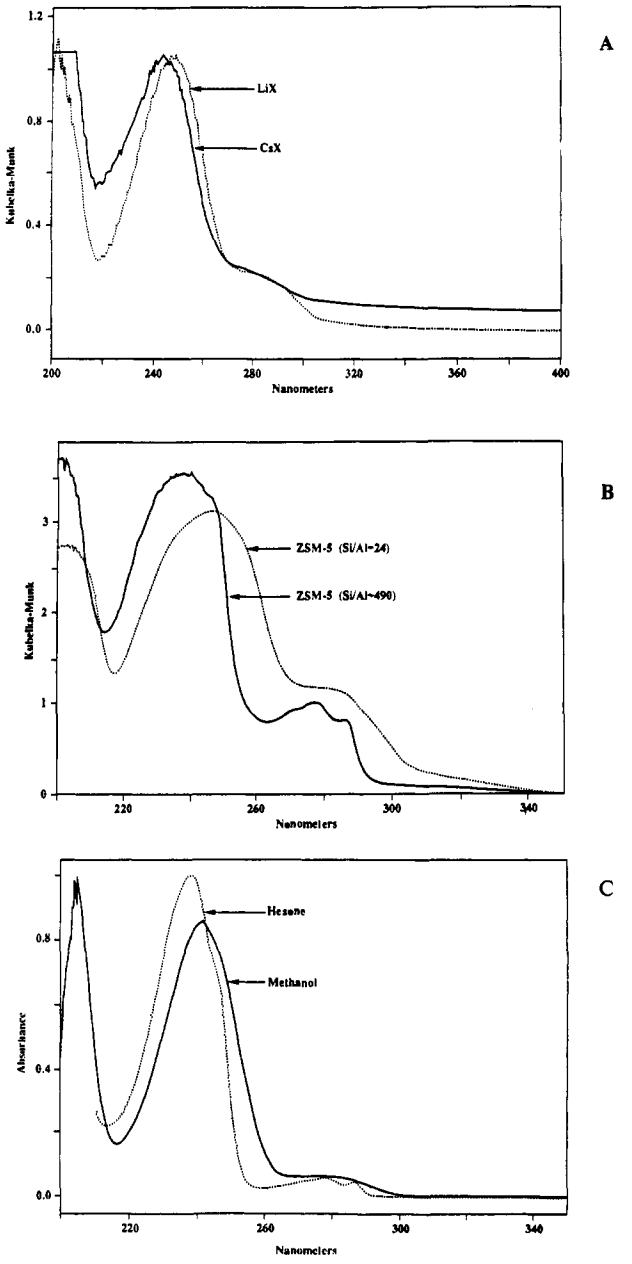

Figure 2. Diffuse reflectance spectra of valerophenone included in Li X and Cs X (A) and in Na ZSM-5 with Si/Al ~ 24 and 490 (B); absorption spectra in hexane and methanol (C).

Steady-State Absorption and Emission Spectra. Diffuse reflectance spectra of the solid zeolite complexes of **1a–f** were recorded at room temperature. Diffuse reflectance spectra of valerophenone (VLP) complexes of Li X, Cs X, ZSM-5 (Si/Al ~ 24), and ZSM-5 (Si/Al ~ 550) are presented in Figure 2A,B. For comparison, absorption spectra of VLP in hexane and methanol are also shown in Figure 2C. It is well-known that the $n\pi^*$ and $\pi\pi^*$ absorption energies as well as the spectral resolution are influenced by the polarity of the medium.[7] Examination of Figure 2B,C reveals a close resemblance between the diffuse reflectance spectra of VLP in Na ZSM-5 (Si/Al ~ 24) and in Na ZSM-5 (Si/Al ~ 490) and the absorption spectra of VLP in methanol and hexane, respectively. In addition to wavelength shifts, the spectral resolution also varied for Na ZSM-5 samples with different Si/Al ratios (Figure 2B). Diffuse reflectance spectra were also recorded for VLP included in Na ZSM-5 zeolites with a number of Si/Al ratios (~24, 34, 67, 120, and 490). Spectra

(7) Ito, M.; Inuzuka, K.; Imanishi, S. *J. Am. Chem. Soc.* **1960**, *82*, 1317. Fendler, J. H.; Fendler, E. J.; Ifante, G. A.; Shih, P. S.; Patterson, L. K. *J. Am. Chem. Soc.* **1975**, *97*, 89.

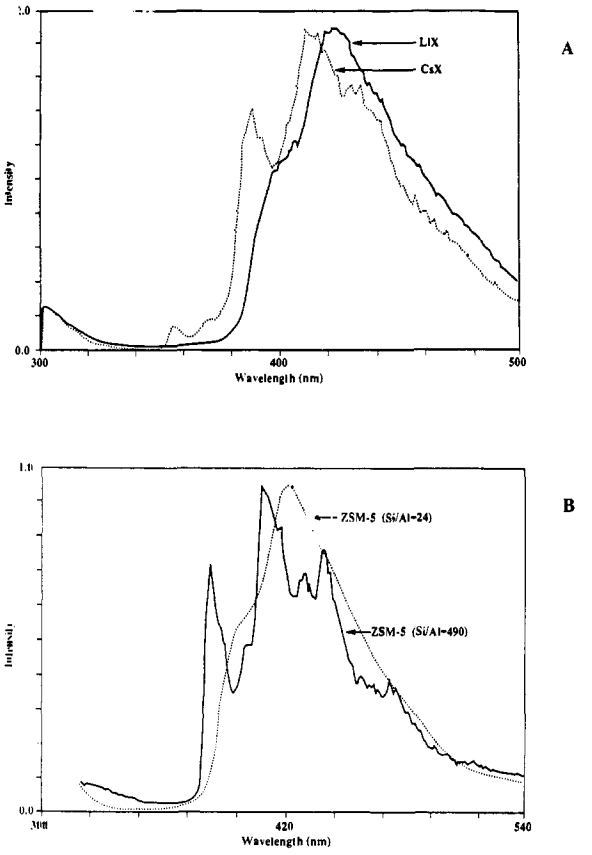

Figure 3. Phosphorescence emission spectra of valerophenone included in Li X and Cs X (A) and in Na ZSM-5 with Si/Al ~ 24 and 490 (B).

of the complexes with Si/Al ratios of ~24, 34, and 67 closely resemble each other, while those with Si/Al ratios of ~120 and ~490 are different from the others but similar to each other. There is a small difference in diffuse reflectance spectral maxima between Li X–VLP and Cs X–VLP complexes (Figure 2A). Spectra of K X and Rb X complexes resemble that of Cs X whereas the maximum for Na X was between those of Li X and Cs X.

Excitation at 77 K (250–300 nm) of valerophenone included in zeolites gave rise to phosphorescence in the region 375–550 nm. The emission spectra of VLP in Li X, Cs X, ZSM-5 (Si/Al ~ 24), and ZSM-5 (Si/Al ~ 550) are displayed in Figure 3. This emission is quenchable, to a certain degree, by oxygen. Perusal of Figure 3 reveals that the emission spectral resolution depends on the cation for the X zeolites and on the Si/Al ratio for the ZSM-5 zeolites. Examination of the excitation spectra shown in Figure 4 reveals considerable differences between Li X and Cs X complexes and between Na ZSM-5 (Si/Al ~ 24 and ~ 490) complexes. In contrast to the diffuse reflectance spectra, absorption due to the $n\pi^*$ transition is readily seen in the excitation spectra. As pointed out by Casal and Scaiano,[5] room temperature phosphorescence is not observed from samples of valerophenone included in the above zeolites. Upon excitation at 260 nm a weak emission in the region 360–470 nm (with an excitation spectrum different from that of valerophenone) is recorded, and this we attribute to emission from the zeolite matrix.

Diffuse Reflectance Laser Flash Photolysis. A. Transient Spectra. Laser excitation (266 nm) of nitrogen-purged samples of VLP on Na ZSM-5 and Cs ZSM-5 generated strongly absorbing transients in the region 300–400 nm. Spectra obtained at low laser intensities (<5 mJ/pulse) and at short delay times after laser excitation are shown in Figure 5 for VLP on the two zeolites. Both show a maximum at ~355 nm and change only in intensity as the delay between the laser pulse and the measurement of the spectrum is increased. The spectra obtained from VLP are almost identical to that of acetophenone (ACP) in Na ZSM-5 (Figure 5C). Purging each of these samples with oxygen

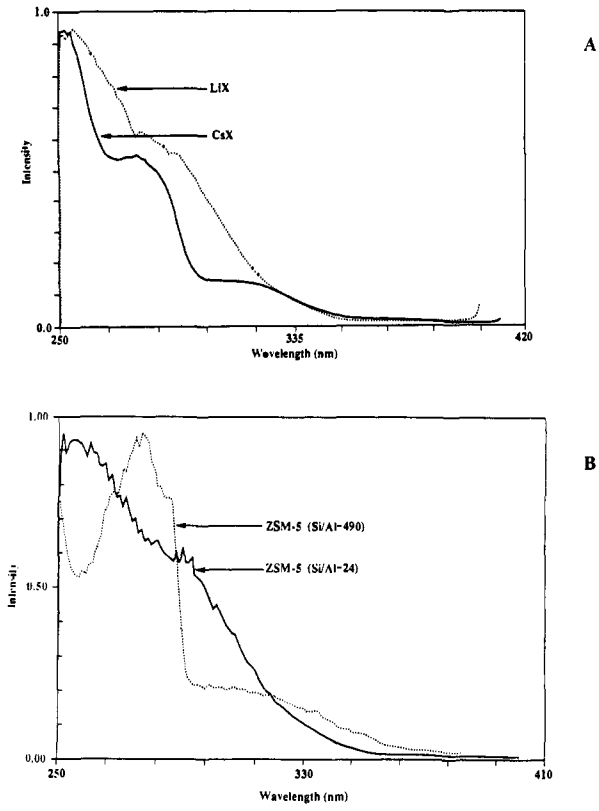

Figure 4. Phosphorescence excitation spectra of valerophenone included in Li X and Cs X (A) and in Na ZSM-5 with Si/Al ~ 24 and 490 (B).

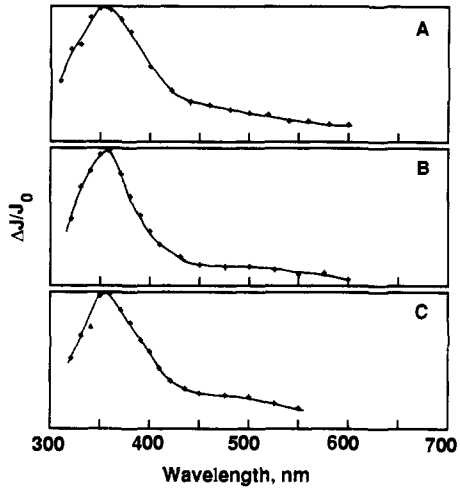

Figure 5. Transient spectra recorded approximately 1 μs after 266-nm excitation of valerophenone in Na ZSM-5 (A) and Cs ZSM-5 (B) and acetophenone in Na ZSM-5 (C).

leads to substantial decreases in the signal intensities and to a more rapid decay of the transient. On the basis of these observations, the observed transients are assigned to the triplet–triplet absorption spectra of VLP and ACP. This assignment is consistent with the fact that similar spectra have been reported for the triplet states of these and related ketones included in silicalite[6] and adsorbed on silica gel.[8] The use of higher laser intensities (>20 mJ) leads to other signals in addition to the triplet–triplet absorption; this effect is much more pronounced in the X zeolites and is discussed in more detail below.

Two transient spectra recorded after 266-nm excitation of VLP in Na X are shown in Figure 6. Spectrum A is recorded at a laser intensity of ~2 mJ and is similar to that measured for VLP

(8) Turro, N. J.; Gould, I. R.; Zimmt, M. B.; Cheng, C. C. *Chem. Phys. Lett.* **1985**, *119*, 484.

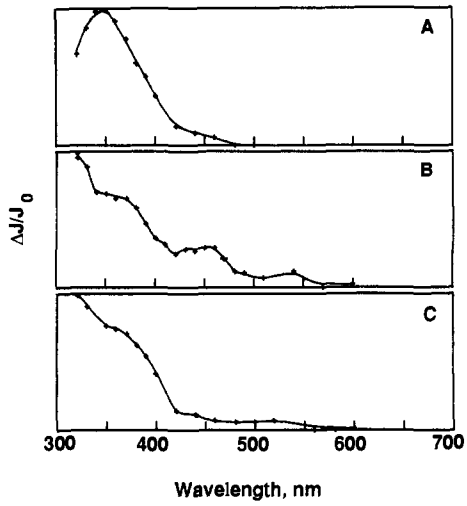

Figure 6. Transient spectra recorded approximately 0.3 μs after 266-nm excitation of valerophenone in Na X at low (A, 2 mJ) and high (B, 20 mJ) laser intensities and of acetophenone in Na X at lower laser intensity (C).

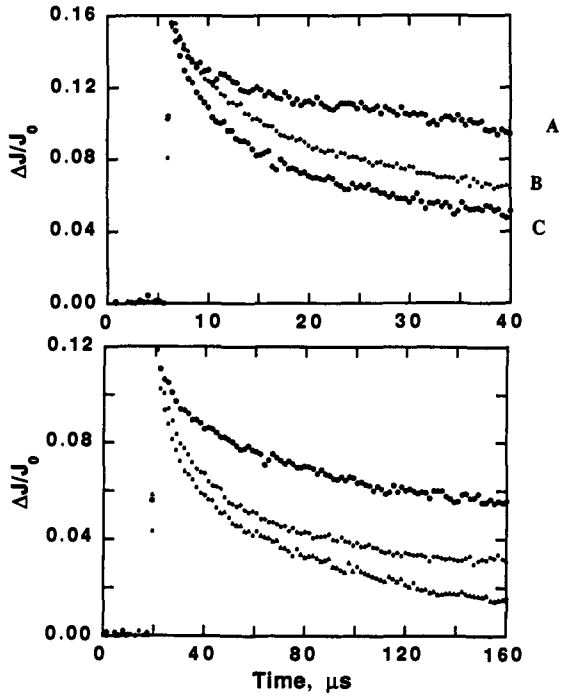

Figure 7. Transient decay traces monitored at 360 nm on two different time scales for acetophenone in Na ZSM-5 (A) and valerophenone in Na ZSM-5 (B) and Cs ZSM-5 (C).

in ZSM-5, consistent with its assignment to triplet VLP. However, at higher laser intensities, the spectrum changes substantially (Figure 6B), and additional absorptions at 450 and 320 nm become evident. The two new bands decay with similar kinetics and are substantially longer lived than the VLP triplet. Similar effects of laser intensity on the transient signals were observed for ACP in Na X, which indicates that the species with absorptions at 450 and 320 nm is not due to the biradical produced by intramolecular hydrogen abstraction. Furthermore, samples of either VLP or ACP which were prepared without the use of a solvent also exhibited this laser-intensity dependence. This rules out the formation of a radical by hydrogen abstraction from residual solvent in the zeolite. Since these control experiments indicated that the unidentified species produced at high laser dose has little to do with the one-photon chemistry of VLP, all further experiments were carried out at low laser intensities where these effects were not observed.

B. Transient Decay. The transient decays for VLP in either Na- or Cs-exchanged ZSM-5 occur over a fairly wide range of

Table II. Decay Kinetics for Triplet Valerophenone in Various Zeolites[a]

zeolites	lifetime (μs)
Li X[a]	4–5
Na X	0.8 ± 0.4[b,c]
K X[a]	0.9 ± 0.4[b]
Rb X[a]	0.7 ± 0.3[b]
Cs X[a]	<0.2
Li Y[d]	0.6
Na Y[d]	0.8
Cs Y[d]	<0.2
Na ZSM-5[a]	28[e]
Cs ZSM-5[a]	14[e]
ZSM-5 (Si/Al 24)[d]	56[e]
ZSM-5 (Si/Al 490)[d]	15[e]

[a] Lifetimes are based on two to three determinations for independently prepared samples. [b] Decay kinetics gave good fits to single exponential kinetics with 5–10% of a residual longer-lived signal. [c] The values for this sample varied from 0.4 to 1.3 for independently prepared samples; values of 0.4, 0.5, 0.62, 0.68, and 0.8 were measured for a set of five samples which were prepared at the same time using exactly the same procedure. [d] Results are based on a single sample. [e] The decay kinetics were multiexponential; numbers quoted correspond to 1 half-life of the triplet.

time scales and do not fit either a single- or double-exponential decay. Such exponential or stretched kinetics are typical of the decays of triplets and other transients in a variety of solid environments.[6,9] Figure 7 shows decay traces which were recorded on two time scales (0.4 and 1.6 μs per point) for VLP in Na ZSM-5 and Cs ZSM-5. For comparison, similar decay traces for ACP on Na ZSM-5 are also shown in Figure 7. The data show that a substantial fraction of the triplets decay within 10–20 μs for each sample, although there are some that decay much more slowly. Further, there are small but reproducible differences between the Na and Cs samples for triplet VLP, with the Cs sample decaying more rapidly. Table II lists data for the triplet decays in several ZSM-5 zeolites as the time required for the signal to decay to $1/e$ of its initial magnitude, as a relative measure of the kinetics. The ACP triplet decays more slowly (half-life of 140 μs) than either of the VLP samples. The decays of triplet VLP for five Na ZSM-5 samples with varying Si/Al ratios (~24, 34, 67, 120, and 490) were also examined. The triplet was somewhat longer lived with increasing aluminum content in the zeolite, but the differences were not large (Table II). These effects are illustrated in Figure 8, which shows decay traces on two time scales for the highest and lowest Si/Al ratios. The decay of triplet VLP included in silicalite was measured in order to compare the present results to those obtained previously.[6] The triplet decay in silicalite (half-life of ~10 μs, nonexponential decay kinetics) was similar to that for VLP in the ZSM-5 sample with a Si/Al ratio of ~490. Triplet ACP in silicalite had a significantly slower decay than did VLP, in agreement with previous results.[6]

The transient decay at 360 nm for a sample of VLP in Na X is shown in Figure 9. In this case, the data can be fit reasonably well with a single exponential, although in some cases there is a small amount (5–10%) of a longer-lived residual. Note that at high laser intensity this residual absorption becomes much larger, due to the presence of the additional long-lived transients referred to above. A single-exponential treatment of the data in Figure 9 leads to a lifetime of ~0.8 μs for the decay of triplet VLP. Although the data for a particular sample are reproducible from one measurement to the next (even when these are several weeks apart), we have observed considerable variation in the measured lifetimes for different samples of VLP on Na X. The numbers varied from 0.4 to ~1.2 μs, even though the same sample preparation procedure was used in each case. Since it was thought that some of these problems resulted from variation in water content from one day to the next, five samples were prepared at

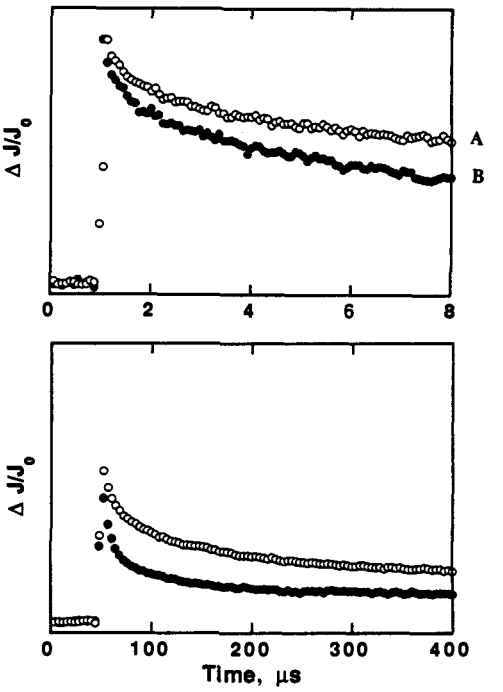

Figure 8. Transient decay traces monitored at 360 nm on two different time scales for valerophenone in ZSM-5 with different Si/Al ratios (Si/Al ~ 24 (A), Si/Al ~ 490 (B)).

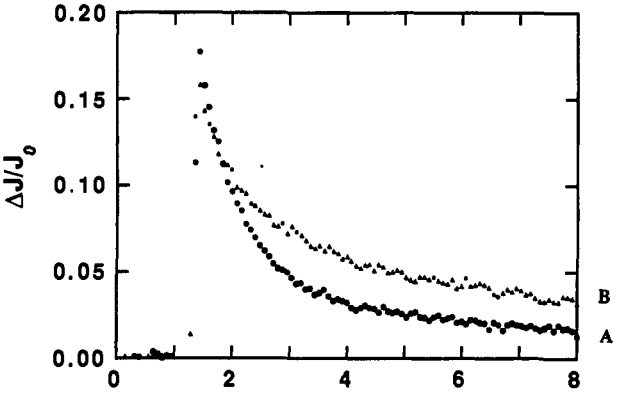

Figure 9. Transient decay traces monitored at 360 nm for valerophenone in Na X (A) and Li X (B).

the same time, using identical materials and procedures. Triplet lifetimes of 0.4, 0.5, 0.62, 0.68, and 0.8 μs were recorded for these samples. These results suggest that it is very difficult to control the reproducibility of the sample preparation procedure.

Samples of VLP in X zeolite exchanged with other cations were also examined. At least two independently prepared samples were studied in each case. The triplet lifetimes for Na, K, and Rb X were all between 0.4 and 1.2 μs (Table II), indicating little effect of the cation, at least within the limitation of the rather large variations in triplet lifetime from one sample to the other. However, there were significant changes when the cation was changed to either Li or Cs. For the Li X samples, the triplet decay was much longer (4–5 μs, Figure 9) and did not give satisfactory fits to a single-exponential decay. However, the initial signal intensity and the triplet–triplet absorption spectrum were not affected by the substitution of Li for Na. On the other hand, samples of VLP in Cs X gave weak signals which decayed in <0.2 μs. Problems with scattered light and luminescence prevented us from examining these samples on short time scales, so we cannot exclude the possibility that much of the signal decayed outside of our detection range.

Samples of VLP in Y zeolites were also examined. In this case, the triplet lifetimes for Li Y and Na Y (Table II) were similar to those recorded for Na X, and Cs Y gave only weak short-lived signals.

(9) Oelkrug, D.; Krabichler, G.; Honnen, W.; Wilkinson, F.; Willsher, C. J. *J. Phys. Chem.* **1988**, *92*, 3589. Draper, R. B.; Fox, M. A. *Langmuir* **1990**, *6*, 1396. Johnston, L. J.; Scaiano, J. C.; Shi, J.-L.; Siebrand, W.; Zerbetto, F. *J. Phys. Chem.* **1991**, *95*, 10018.

Table III. Photolysis of Aryl Alkyl Ketones in Various Zeolites: Dependence of Product Distribution on the Internal Structure of Zeolites[a-c]

medium	butyrophenone (**1a**) E/C	valerophenone (**1b**) E/C	octanophenone (**1c**) E/C	octanophenone (**1c**) CB_t/CB_c	dodecanophenone (**1d**) E/C	dodecanophenone (**1d**) CB_t/CB_c	tetradecanophenone (**1e**) E/C	tetradecanophenone (**1e**) CB_t/CB_c	octadecanophenone (**1f**) E/C	octadecanophenone (**1f**) CB_t/CB_c
hexane	8.8	2.8	1.8	3.1	1.8	2.8	3.5	2.7	1.9	3.0
benzene	8.3	2.7	1.9	2.5	1.4	2.4	1.8	2.4	1.4	2.6
methanol	13.6	3.5	3.4	2.0	1.3	1.7	1.6	1.5	3.9	1.8
Na X	3.0	1.2	0.9	1.0	0.6	0.6	0.5	0.8	1.0	1.2
Na Y	3.2	1.1	0.6	1.0	0.5	0.7	0.2	1.2	0.5	1.3
LZ-L	4.5	2.1	2.3	0.7	0.8	0.5	0.6	0.5	1.1	1.1
Na Ω-5	11	4.6	2.5	1.6	2.5	1.6	4.0	1.2	2.7	1.8
Na M-5	5.4	3.2	1.8	1.1	6.2	1.0	2.2	0.7	1.3	1.5
offretite	5.4	26	only E	–	only E	–	only E		only E	
ZSM-34	only E	only E	only E	–	only E	–	only E		only E	
ZSM-5	73	only E	only E	–	only E	–	only E		only E	
ZSM-11	56	only E	only E	–	only E	–	only E		only E	
θ-1		none of these ketones were adsorbed								
Na, 4A		none of these ketones were adsorbed								

[a] Analyzed by GC using SE-30 capillary column; numbers reported are the average of at least four independent runs assuming identical detector response; error limit, ±5%; conversion in all cases was maintained at less than 15%. Product distribution was independent of the conversion in the range 10–60%. [b] E/C corresponds to the ratio of acetophenone to cyclobutanols; CB_t/CB_c represents the ratio of *trans*- to *cis*-cyclobutanols. The *trans*-cyclobutanol had a longer retention time than the cis isomer on the above column; however, the reverse was the case during silica gel flash chromatography. [c] Loading level in all cases was about 5 mg of ketone in 250 mg of zeolite.

Table IV. Photolysis of Aryl Ketones in Various Cation-Exchanged X and Y Zeolites[a-c]

medium	butyrophenone (**1a**) E/C	valerophenone (**1b**) E/C	octanophenone (**1c**) E/C	octanophenone (**1c**) CB_t/CB_c	dodecanophenone (**1d**) E/C	dodecanophenone (**1d**) CB_t/CB_c	tetradecanophenone (**1e**) E/C	tetradecanophenone (**1e**) CB_t/CB_c	octadecanophenone (**1f**) E/C	octadecanophenone (**1f**) CB_t/CB_c
Li X	3.9	1.3	1.6	2.6	0.6	1.4	0.3	1.4	0.9	1.7
Na X	2.7	1.1	1.0	1.0	0.5	0.8	0.5	0.8	1.0	1.2
K X	3.3	1.1	1.9	1.1	0.6	1.1	0.4	1.3	1.5	2.0
Rb X	1.9	1.6	1.9	1.6	0.7	4.5	0.5	2.2	3.0	2.2
Cs X	2.3	1.3	1.9	3.2	1.2	6.8	0.3	5.1	2.5	5.0
Li Y	5.0	1.0	0.6	1.3	0.5	1.3	0.4	1.7	0.6	1.5
Na Y	3.2	1.1	0.5	1.0	0.4	0.9	0.2	1.2	0.5	1.3
K Y	2.8	1.5	0.6	1.0	0.5	1.1	0.4	1.1	0.5	1.6
Rb Y	2.5	1.2	0.5	1.0	0.6	1.4	0.2	1.2	0.4	1.6
Cs Y	1.1	0.6	0.8	1.2	0.5	1.3	0.3	1.7	0.4	1.6
Na X (slurry)[d]	3.7	0.3	0.1	3.1	0.01	1.0	0.1	0.9	0.01	1.2
K X (slurry)[d]	1.4	0.2	0.07	2.9	0.01	1.3	0.02	1.7	0.01	1.6
Na Y (slurry)[d]	0.5	0.02	0.02	0.9	0.01	0.6	0.01	0.8	0.01	0.7
K Y (slurry)[d]	0.3	0.04	0.01	3.2	0.01	1.2	0.01	1.4	0.01	1.8

[a] Analyzed by GC using SE-30 capillary column; numbers reported are the average of at least four independent runs assuming identical detector response; error limit, ±5%; conversion in all cases was maintained at less than 15%. Product distribution was independent of the conversion in the range 10–60%. [b] E/C corresponds to the ratio of acetophenone to cyclobutanols; CB_t/CB_c represents the ratio of *trans*- to *cis*-cyclobutanols. [c] The loading level was approximately 0.2. Ketone amount was about 5 mg in all cases. The weight of zeolite varied between 250 and 400 mg. Note that to have the same number of cages one has to use a higher amount of Cs X than Na X. [d] Zeolite–hexane slurry.

Photolysis. Aryl alkyl ketones **1a–f** were irradiated (in degassed and sealed Pyrex tubes) as complexes of zeolites at room temperature. The loading level in all cases was much below the saturation limit. Most of the ketone molecules, for reasons outlined in the Discussion, are believed to be adsorbed on the inner rather than on the outer surface of the zeolite. Sample preparation ensured that the molecules adsorbed outisde were washed away by the solvent. Table III summarizes the results of product distributions obtained in the various zeolites. The elimination to cyclization ratio corresponds to the ratio of acetophenone to cyclobutanol (cis and trans) yields (Scheme I). Ratios of *cis*- to *trans*-cyclobutanols are also provided. For comparison, product distributions obtained under our conditions in hexane, benzene, and methanol are also listed. Perusal of Table III indicates that the product distribution differs dramatically between large-pore (X, Y, L, Ω-5, and M-5) and medium-pore (ZSM-5, -11, and -34 and offretite) zeolites. For all the ketones except butyrophenone, the cyclization process is prevented within the cages and channels of the medium-pore zeolites. Further, small but significant differences in product distribution are noted between various zeolites, especially with butyrophenone. In order to assess the role of cations in controlling the course of Norrish type II reactions of **1**, photolyses of **1** in X and Y zeolites with Li, Na, K, Rb, and Cs as cations were carried out. The results are provided in Table IV. While the elimination to cyclization (E/C) ratios are not significantly affected by the nature of the cation, the ratio of *cis*- to *trans*-cyclobutanols shows some dependence on the cation, particularly in the case of X zeolites.

One can control the free volume available for the guest molecule within a cage by incorporating inert molecules such as solvent along with the guest ketone.[10] With this in mind, we conducted the photolyses of **1a–f** in Na X and Na Y as hexane slurries and as dry complexes under identical conditions. Under our loading conditions, all the ketone remained within the zeolite in the zeolite–hexane preparations, as confirmed by GC analysis and UV absorption of the hexane layer. All the products reported in Table IV for zeolite-slurry irradiations are derived from ketones reacting within the zeolites. A comparison between solid and zeolite–hexane slurry irradiations reveals that the E/C ratio is much lower in the presence of hexane within the cage. Irradiation of **1a–f** at several different loading levels ($\langle S \rangle$ between 0.01 and 0.5) in Na X was conducted. Neither the E/C nor the *trans*- to *cis*-cyclobutanol ratio varied with loading level.

The above studies indicate that the product distribution is a function of the zeolite structure, the nature of the cation, and the presence of inert filler. To probe whether the above dependence is also seen in the efficiency of product formation, relative quantum yields of type II product formation were measured for VLP in various zeolites. The ketone concentration was identical in all

(10) Turro, N. J. *Pure Appl. Chem.* **1986**, *58*, 1219. Turro, N. J.; Cheng, C. C.; Lei, X. G.; Flanigen, E. *J. Am. Chem. Soc.* **1985**, *107*, 3740.

Table V. Photolysis of Valerophenone in Various Zeolites: Relative Quantum Yields of Type II Product Formation[a,b]

zeolites	relative Φ_{II}
Li X	1.00
Na X	1.8
K X	2.2
Rb X	2.6
Cs X	3.4
Li Y	1.0
Na Y	1.0
K Y	2.3
Rb Y	5.6
Cs Y	7.6
ZSM-5 (Si/Al 32)	0.4

[a] All samples had identical amounts of ketone. Products were analyzed by GC with *trans*-stilbene as the internal standard. Numbers reported above are the average of three independent measurements. Amounts of both acetophenone and cyclobutanols were measured. [b] Irradiations were conducted in two sets: X series and ZSM-5, and Y series. Relative Φ_{II} are comparable within the X series and Y series. ZSM-5 should be compared with the X series.

cases, and the diffuse reflectance spectra were almost the same for all these samples. The results, summarized in Table V, were obtained by photolysis of these optically matched samples for the same length of time under identical conditions. The numbers have been normalized with respect to Li X and Li Y. The errors in these measurements are expected to be larger than those in the product-yield determinations due to the difficulty in ensuring that the same amount of light is absorbed by each sample. However, it is clear that the relative quantum yield depends on the cation and on the nature of zeolite.

Discussion

Location of Ketone Molecules within Zeolites. In order to interpret the experimental results, one requires some knowledge concerning the location of the guest ketones adsorbed within the zeolites. Of the two possible locations, internal and external surfaces, we believe that adsorption occurs on the internal surface for the following reasons: (a) The available external surface area is much smaller (<1%) than the internal surface area. (b) No significant amount of ketone is adsorbed onto zeolites with too small a pore diameter to admit these molecules (e.g., zeolites 4A and θ, Table I and III). (c) The photochemical behavior of valerophenone within zeolites is significantly different from that on silica gel;[8] had the molecules been adsorbed on the external surface of the zeolites, one might anticipate behavior similar to that on a silica gel surface. (d) Differences in product distribution are obtained between zeolites; had the photoreaction been occurring on the outside surface, no such variation would be expected. (e) The adsorption isotherms for valerophenone suggest that the maximum amount of guest adsorbed is related to the internal free volume since both the internal free space and the maximum amount of ketone adsorbed decrease in the order Li X, K X, and Cs X.

The exact position of guests within zeolites cannot be obtained via X-ray structural studies as all guest molecules are mobile within the channels, cages, and cavities of zeolites at room temperature. However, other techniques have been used to determine the location of small guest molecules such as benzene, *p*-xylene, and pyridine.[11] It is clear from these studies that the cation plays a key role in determining the location of guests within X, Y, ZSM, β, L, and mordenite zeolites. Indirect evidence favoring the cation sites as the location of aryl alkyl ketones in X and Y zeolites comes from our IR studies and thermogravimetric analyses. The carbonyl stretching frequency of valerophenone shows cation dependence: Na X, 1651 cm^{-1}; Cs X, 1675 cm^{-1}; and neat, 1687 cm^{-1}. A similar dependence which may also have its origin in the cation interaction is seen in the case of ZSM-5 zeolites: ZSM-5 (Si/Al $\sim$ 24), 1665 cm^{-1}; ZSM-5 (Si/Al $\sim$ 490), 1690 cm^{-1}. Indeed, thermogravimetric analyses of octanophenone–zeolite complexes indicate the presence of an interaction between the cation and the ketone. For example, the temperatures of desorption of octanophenone adsorbed over Y and ZSM-5 zeolites as measured by thermogravimetric analyses were found to be Li Y, 407 °C; K Y, 391 °C; Cs Y, 341 °C; ZSM-5 (Si/Al $\sim$ 24), 330 °C; and ZSM-5 (Si/Al $\sim$ 490), 291 °C. It is known[4] that a stronger interaction between the cation and the adsorbent leads to a higher desorption temperature. Thus, the strength of the binding interaction would be expected to follow the trend $Li^+ > K^+ > Cs^+$.

A comparison between solution and zeolite diffuse reflectance and emission spectra (Figures 2 and 3) also provides some information on the relationship between the cation and the guest ketones. The shift in λ_{max} and the spectral resolution of the diffuse reflectance and emission spectra indicate that the microenvironment of the guest ketone is more polar in the case of Li X than in Cs X. Similarly, VLP experiences a higher micropolarity in the channels of ZSM-5 with Si/Al $\sim$ 24 than in the channels of ZSM-5 with Si/Al $\sim$ 490. Micropolarity within zeolites may not have the same meaning as in solution and is quite likely a reflection of the electric field generated by the cation. A higher electric field due to the cation would imply a higher micropolarity. It has been estimated that the electrostatic potential and electric field within the cage depend on the charge density or electronegativity of the cation.[12a] Indeed, the micropolarity of the zeolite X and Y supercage as monitored with pyrene, 1-pyrenecarboxaldehyde, and 4-(dimethylamino)benzonitrile was found to depend on the cation.[12b] The micropolarity within Li X was comparable to that of the methanol–water mixture, while that of Cs X was comparable to that of propanol. Zeolites with Na, K, and Rb as cations were found to possess intermediate polarity. Therefore, we believe that the shifts and changes in spectral resolution in the diffuse reflectance and excitation spectra of the included ketones reflect the nature of the interaction between the cation and guest molecule. On the basis of all these observations, we conclude that the reactive ketones are located within the internal surface of zeolites in close proximity to the cations.

Distribution of Ketone Molecules within Zeolites. The distribution of ketone molecules within zeolites may or may not be uniform. This also means that the microenvironment around the guest molecules within a zeolite may not be uniform. The inhomogeneity in the microenvironment experienced by a guest can arise for two reasons: (a) variation in the occupancy number within a cage or channel and (b) the presence of sites of varying microenvironment within the zeolite lattice. Even at low loading levels the cages may not be uniformly occupied, i.e., some may be singly occupied, some multiply occupied, and others empty. By utilizing pyrene, *trans*-stilbene, and 1-pyrenecarboxaldehyde as probes, we have come to the conclusion that there is a wide range of possible sites or environments for guest molecules within the zeolite interior.[13] Therefore, it is quite likely that even in the systems described here not all ketone molecules experience an identical environment. This is indeed reflected in the nonexponential triplet decays for valerophenone, particularly for the ZSM-5 samples. However, the presence of multiple sites was not evident in the emission spectra of VLP in ZSM-5 and Na X. The spectral shape, the resolution, and the wavelength region of emission were independent of the excitation wavelength.

(11) For a few recent references, see: de Mallman, A.; Barthomeuf, D. *Zeolites* **1988**, *8*, 292. de Mallman, A.; Barthomeuf, D. *J. Chem. Soc., Chem. Commun.* **1989**, 129. de Mallman, A.; Dzwigaj, S.; Barthomeuf, D. In *Zeolites: Facts, Figures, Future*; Jacobs, A., van Santen, R. A., Eds.; Elsevier: Amsterdam, 1989; p 935. O'Malley, P. J. *Chem. Phys. Lett.* **1990**, *166*, 340. Ryoo, R.; Liu, S. B.; de Menorval, L. C.; Takegoshi, K.; Chmelka, B.; Trecoske, M.; Pines, A. *J. Phys. Chem.* **1987**, *91*, 6575. de Menorval, L. C.; Raftery, D.; Liu, S. B.; Takegoshi, K.; Ryoo, R.; Pines, A. *J. Phys. Chem.* **1990**, *94*, 27. Fitch, A. N.; Jobic, H.; Renouprez, A. *J. Chem. Soc., Chem. Commun.* **1985**, 284. Fitch, A. N.; Jobic, H.; Renouprez, A. *J. Phys. Chem.* **1986**, *90*, 1311. Czjek, M.; Vogt, T.; Fuess, H. *Angew. Chem., Int. Ed. Engl.* **1989**, *28*, 770. Jobic, H.; Renouprez, A.; Fitch, A. N.; Lauter, H. J. *J. Chem. Soc., Faraday Trans. 1* **1987**, *83*, 3199. de Mallmann, A.; Barthomeuf, D. *J. Phys. Chem.* **1989**, *93*, 5636.

(12) (a) Ward, R. J. *J. Catal.* **1968**, *10*, 34. (b) Ramamurthy, V.; Sanderson, D. R.; Eaton, D. F. *Photochem. Photobiol.*, in press.

(13) Ramamurthy, V.; Caspar, J. V. *Mol. Cryst. Liq. Cryst.* **1992**, *211*, 211.

Scheme II

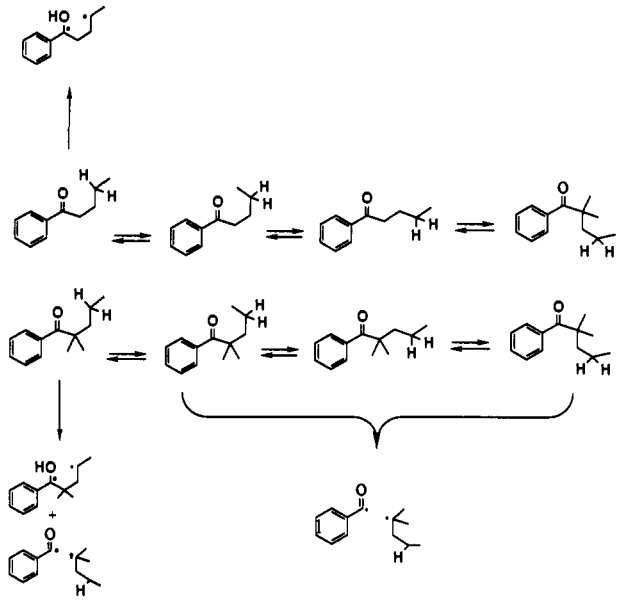

Decay of Valerophenone Triplet, Efficiencies of Product Formation, and Conformational Equilibrium. Several aspects of the results on VLP triplet decay in zeolites need to be addressed. The first of these is the large increase in triplet lifetime for VLP in zeolites (microseconds) with respect to that in homogeneous solution (~5 ns).[14] The triplet lifetime of VLP in zeolites is controlled predominantly by intramolecular hydrogen abstraction. This is made evident by the measured lifetime of acetophenone in X and ZSM-5 zeolites. Acetophenone, which decays only through photophysical processes, has a considerably long lifetime when compared to that of VLP in both X and ZSM-5 zeolites. The long triplet lifetime, a consequence of reduced rate of γ-hydrogen abstraction, observed for VLP in both X and ZSM-5 zeolites might arise due to one or both of two factors: (a) a change in the character of the lowest triplet ($n\pi^*$ and $\pi\pi^*$)[15] and (b) a change in the conformer distribution of the reactive and the nonreactive conformers (Scheme II).[16] The effect of solvent polarity and substituents on triplet-state switching and state mixing ($n\pi^*$ and $\pi\pi^*$) have been well documented.[15] Electron-donating substituents and polar solvents favor the $\pi\pi^*$ triplet as the lowest state. We reason below that observed long triplet lifetime in zeolites is a consequence of the above two factors. The cation in the case of faujasites and the ratio of silicon to aluminum in the case of pentasils appear to influence the extent of individual contribution by the above two factors. Examination of Table II reveals that the triplet lifetime is considerably long when lithium is the cation. It is important to note that the strength of binding interaction between the carbonyl and the cation is dependent on the cation and has been shown to be strong in the case of lithium (see above). Therefore, it is quite likely that the long lifetime observed in Li X is a consequence of the change in the character of the lowest triplet from $n\pi^*$ to $\pi\pi^*$. Such a proposal is supported by the phosphorescence spectra. Examination of Figure 3 reveals that the emission observed in Li X is distinctly different from that in Cs X. While the emission in Li X is characteristic of a $\pi\pi^*$, that in Cs X is characteristic of an $n\pi^*$ state.[15] Such a reversal in the character of the lowest triplet in polar solvents has been reported earlier. The interior of Li X being more polar[12b] than other cation-exchanged X zeolites, such a reversal is not unexpected. A similar reasoning leads us to conclude that VLP in ZSM-5 with high aluminum content (Si/Al ~ 24) has the lowest triplet of $\pi\pi^*$ character. Long triplet lifetime, poorly resolved phosphorescence (Figure 3), and diffuse reflectance spectra resembling that of absorption in methanol (Figure 2) are all in common with those discussed above for VLP included in Li X. Therefore, we conclude that the long lifetime observed for VLP in Li X and in ZSM-5 (Si/Al ~ 24) is a result of the lowest triplet having $\pi\pi^*$ character. Under such conditions γ-hydrogen abstraction must be occurring from a thermally populated $n\pi^*$ triplet state lying nearby.[1] The change in the character of the lowest triplet cannot be responsible for the relatively long lifetime (with respect to solution) of VLP in other cation-exchanged zeolites and in ZSM-5 with high silicon content. These zeolites being less polar, and the cations being not highly interactive with the carbonyl chromophore, a reversal in $n\pi^*$–$\pi\pi^*$ state is not expected.

From Figure 3 it is clear that the phosphorescence emission of VLP in ZSM-5 (Si/Al ~ 490) and in Cs X is characteristic of an $n\pi^*$ state. Furthermore, diffuse reflectance spectra of VLP in these zeolites resemble that in hexane (Figure 2). The interiors of ZSM-5 (Si/Al ~ 490) and Cs X have been shown to be nonpolar by the probe 4-(dimethylamino)benzonitrile.[12b] This is consistent with the observed similarity in the diffuse reflectance spectrum of VLP in these zeolites and the absorption spectrum in hexane (Figure 2B,C). On the basis of previous investigations in isotropic media,[15] one would expect the VLP triplet to have $n\pi^*$ character in a relatively nonpolar medium such as above. If this be the case, what contributes to the long lifetime? The observed rate of hydrogen abstraction includes a factor which describes the equilibrium fractional population of favorable conformers.[16] As illustrated in Scheme II, valerophenone exists in a number of conformations, only a few of which are suitable for hydrogen abstraction. Although in solution the conformational equilibrium is fast with respect to hydrogen abstraction, this need not be the case within zeolite cages. Therefore, one can visualize two situations: one in which the conformational equilibrium is achieved within the excited-state lifetime, and a second in which the conformational equilibrium is slow with respect to the triplet decay.[17] Since, as pointed out earlier, the triplet lifetime of VLP in zeolites is controlled by a hydrogen abstraction process, even the nonreactive conformers must be relaxing via the reactive conformers. The decreased rate of hydrogen abstraction, then, must be due to reduced population of the reactive conformer within the zeolite interior. The results shown in Table II indicate that there are substantial differences in triplet lifetime between the X and ZSM-5 zeolites. These results suggest that the narrow channels of the ZSM-5 zeolite impose more severe restrictions on the VLP triplet than do the relatively large cages of the X zeolites. Comparison of our results with the 310-ns lifetime reported for triplet VLP on silica[8] indicates that the supercages of X and Y zeolites do not provide much more restriction than does a silica surface. There is a considerable decrease in lifetime in going from Li to Cs X, with intermediate (and similar) values for Na, K, and Rb (Table II). We tentatively conclude that the extent of favorable conformation required for hydrogen abstraction present in the X and Y zeolites varies with the cation. Such a variation probably arises from differences in the binding ability of the cation. The above rationale led us to investigate the photochemistry of aryl alkyl ketones which can undergo both the type I and the type II processes. As illustrated in Scheme II, α,α-dimethylvalerophenone also exists in a number of conformations similar to valerophenone. In this case, conformations which are not suitable for the type II process can decay via a second chemical process (type I reaction). If the equilibrium conformer distribution is influenced by the cation and by the size and shape of the zeolite interior, one would expect the type I to type II product ratio to vary with the zeolite and the cation. This

(14) Small, R. D.; Scaiano, J. C. *J. Phys. Chem.* **1977**, *81*, 2126. Caldwell, R. A.; Majima, T.; Pac, C. *J. Am. Chem. Soc.* **1982**, *104*, 629. Lissi, E. A.; Encinas, M. V. In *Handbook of Organic Photochemistry*; Scaiano, J. C., Ed.; CRC Press: Boca Raton, 1989; Vol. II, p 111.

(15) Baum, E. J.; Wan, J. K. S.; Pitts, J. N. *J. Am. Chem. Soc.* **1966**, *88*, 2652. Kearns, D. R.; Case, W. *J. Am. Chem. Soc.* **1966**, *88*, 5087. Lamola, A. A. *J. Chem. Phys.* **1967**, *47*, 4810. Wagner, P. J.; Kemppainen, A. E.; Schott, H. *J. Am. Chem. Soc.* **1973**, *95*, 5604.

(16) Lewis, F. D.; Johnson, R. W.; Ruden, R. A. *J. Am. Chem. Soc.* **1972**, *94*, 4292. Lewis, F. D.; Johnson, R. W.; Johnson, D. E. *J. Am. Chem. Soc.* **1974**, *96*, 6090. Lewis, F. D.; Johnson, R. W.; Kory, D. R. *J. Am. Chem. Soc.* **1974**, *96*, 6100. Padwa, A.; Alexander, E.; Niemcyzk, M. *J. Am. Chem. Soc.* **1969**, *91*, 456.

(17) Wagner, P. J. *Acc. Chem. Res.* **1983**, *16*, 461.

Scheme III

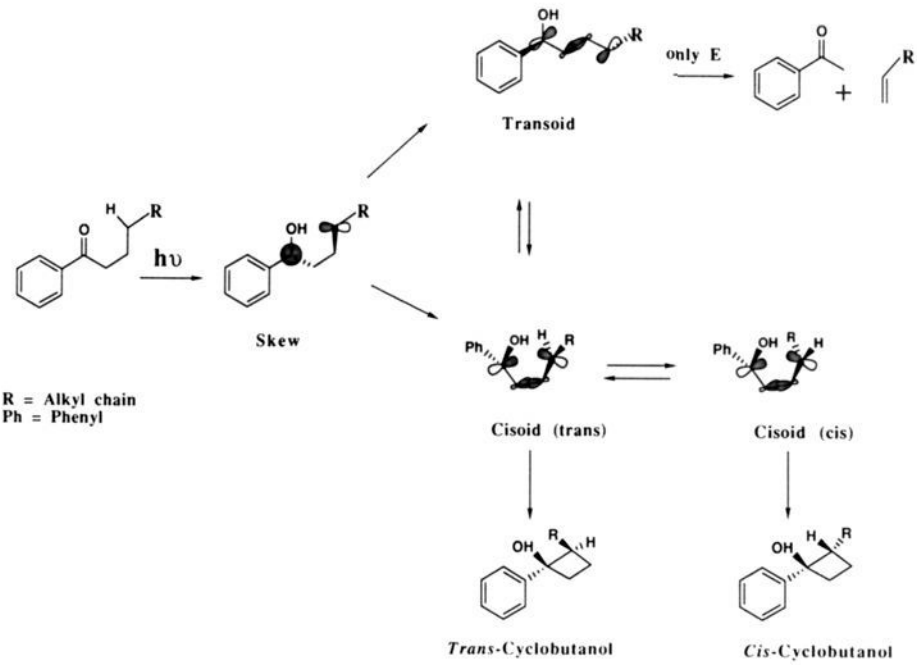

has been found to be the case with a large number of ketones.[18] We believe, therefore, that the equilibrium conformer distribution is influenced by the cation and by the size and shape of the zeolite interior.

Although the triplet lifetimes and the efficiencies of product formation (Table V) both show the same trend with respect to the cation and the nature of zeolites, there is no quantitative correlation between the two. In fact such is not expected.[1] The observed variations in the efficiency of type II product formation are related to the fact that the product yields depend on the competition between the decay of the biradical via cyclization and elimination and the back hydrogen transfer (biradical partitioning) yielding the reactant ketone. It has been established that back hydrogen transfer is the major reaction of the 1,4-diradical in nonpolar solvents. Such a process will decrease the efficiency of the type II product formation. Examination of Table V reveals that the relative efficiency of product formation increases as the electrostatic potential of the cation decreases. It has been established that the cage becomes less polar as the electrostatic potential of the cation decreases. It is indeed comforting to see a qualitative linear relationship between the polarity and the efficiency of type II product formation. Quantitative correlation cannot be made in the absence of absolute quantum yield measurements.

Mechanistic Background. The Norrish type II reaction of aryl alkyl ketones has been extensively investigated, and the mechanistic details are fairly well understood.[1,19] The triplet 1,4-diradical, the primary product of γ-hydrogen abstraction, is generated in the skew form and transforms to the transoid and cisoid conformers via a rotation of the central σ-bond (Scheme III).[20] These geometries are also well suited for intersystem crossing to the corresponding singlet diradical which precedes product formation. As illustrated in Scheme III, these cisoid and transoid conformers undergo further reaction to yield cyclobutanol, olefin, and enol as final products. While the cisoid conformer reacts via both elimination and cyclization processes, the transoid conformer undergoes only elimination.[21,22] It is well-known that in hydrogen-bonding media the decay of the 1,4-diradical is affected by the hydrogen bonding.[23] This is readily seen as the difference in product distributions between hexane and alcohol.

The skew diradical can also directly give rise to products via elimination and cyclization processes, and this is determined by how easily the required orbital overlap can be attained and by how readily the accompanying atomic motions can be tolerated by the medium and by the molecular architecture. Efficient cleavage requires a 1,4-diradical conformation in which both the singly occupied p orbitals can overlap significantly with the central σ-bond being broken.[24] While cyclization prefers the same extensive overlap, it can also be initiated from a geometry involving small nonbonded interactions and partial orbital overlap between the lone p orbitals.[25] Under such conditions, a puckered cyclobutane ring is generated. Cyclization requires considerable atomic displacement of the substituents present on C_1 of the skew diradical; both aryl and hydroxyl groups must move through a large volume.[26] From the above established mechanistic conclusions, it is clear that one can understand the influence of the "microenvironment" on the type II cyclization and elimination processes on the basis of the medium effect on the equilibrium distribution of the cisoid and transoid 1,4-diradical conformers and on the decay of the cisoid and skew conformers.

The stereochemistry of the cyclobutanols (cis and trans) is determined by the population and decay of the two cisoid biradicals

(18) Ramamurthy, V.; Corbin, D. R.; Turro, N. J.; Sato, Y. *Tetrahedron Lett.* **1989**, *30*, 5829. Ramamurthy, V.; Lei, X. G.; Turro, N. J.; Lewis, T. J.; Scheffer, J. R. *Tetrahedron Lett.* **1991**, *32*, 7675.

(19) Wagner, P. J. *Top. Curr. Chem.* **1976**, *66*, 1. Wagner, P. J. In *Molecular Rearrangements in the Ground and Excited States*; de Mayo, P., Ed.; Wiley-Interscience: New York, 1980; p 381. Scaiano, J. C.; Lissi, E. A.; Encina, M. V. *Rev. Chem. Intermed.* **1978**, *2*, 139.

(20) Yang, N. C.; Yang, D. H. *J. Am. Chem. Soc.* **1958**, *80*, 2913. Wagner, P. J.; Hammond, G. S. *J. Am. Chem. Soc.* **1966**, *88*, 1245. Coulson, D. R.; Yang, N. C. *J. Am. Chem. Soc.* **1966**, *88*, 4511. Wagner, P. J.; Kelso, P. A.; Zepp, R. G. *J. Am. Chem. Soc.* **1972**, *94*, 7480.

(21) Caldwell, R. A.; Dhawan, S. N.; Majima, T. *J. Am. Chem. Soc.* **1984**, *106*, 6454. Sonawane, H. R.; Nanjundiah, B. S.; Rajput, S. I.; Kumar, M. V. *Tetrahedron Lett.* **1986**, *27*, 6125. Treanor, R. L.; Weiss, R. G. *Tetrahedron* **1987**, *43*, 1371.

(22) Johnston, L.; Scaiano, J. C.; Sheppard, J. W.; Bays, J. P. *Chem. Phys. Lett.* **1986**, *124*, 493. Ariel, S.; Evans, S. V.; Garcia-Garibay, M.; Harkness, B. R.; Omkaram, N.; Scheffer, J. R.; Trotter, J. *J. Am. Chem. Soc.* **1988**, *110*, 5591.

(23) Wagner, P. J. *Tetrahedron Lett.* **1967**, 1753. Wagner, P. J. *J. Am. Chem. Soc.* **1967**, *89*, 5898.

(24) Wagner, P. J.; Kemppainen, A. E. *J. Am. Chem. Soc.* **1968**, *90*, 5896. Weiss, D. S.; Turro, N. J.; Dalton, J. C. *Mol. Photochem.* **1970**, *2*, 91. Gagosian, R. B.; Dalton, J. C.; Turro, N. J. *J. Am. Chem. Soc.* **1970**, *92*, 4752.

(25) Wagner, P. J.; Kelso, P. A.; Kemppainen, A. E.; McGrath, J. M.; Schott, H. N.; Zepp, R. G. *J. Am. Chem. Soc.* **1972**, *94*, 7506. Lewis, F. D.; Hillard, T. A. *J. Am. Chem. Soc.* **1972**, *94*, 3852.

(26) Ariel, S.; Ramamurthy, V.; Scheffer, J. R.; Trotter, J. *J. Am. Chem. Soc.* **1983**, *105*, 6959.

depicted in Scheme III. Generally, the *trans*-cyclobutanol is the major product in isotropic solvents. However, the ratio of *trans*- to *cis*-cyclobutanol decreases with the increases in the polarity or hydrogen-bonding ability of the solvent. This is attributed to the steric bulk of the hydrogen-bonded hydroxyl group which impedes trans cyclization.[27] Thus, the effect of the zeolite environment on the type II product distribution can be understood on the basis of its effect on the diradical intermediates.

Effects of the Shape and Size of the Reaction Cavity on the Type II Product Distribution. The reaction cavity concept which has been useful in qualitatively understanding the course of a variety of solid-state reactions should be of considerable help in visualizing reactions that occur in organized structures.[28] The reaction cavity is the space occupied by the reacting partners and the empty region surrounding them. The atomic movements which accompany the reaction exert pressures on the cavity wall, which becomes distorted. The tolerance of the cavity wall to these pressures can play an important role in the selectivity of a reaction in a particular medium. Differences in product selectivity obtained for a particular reaction in various media can be attributed to the size, shape, and nature (texture or flexibility) of the reaction cavity available for the reactant molecules. One can define the texture of the reaction cavity as hard or soft depending on whether the molecules which form the wall can undergo some motion to allow the distortion of the reaction cavity. For example, crystals provide a hard reaction cavity, whereas micelles provide a soft one. If one can control and provide a well-defined, small and flexible cavity that can accommodate the reactant molecule with some void space around it, one may predict that a large number of molecules will undergo selective phototransformations in various organized media. It is in this context that zeolites which crystallize with well-defined internal structures consisting of channels, cages, and cavities have been valuable. The internal structures of the zeolites that we have utilized as media for the type II process vary in size and shape (Table I) and thus provide reaction cavities of different geometries. The reaction cavities of the zeolites are expected to be "hard" in the sense that they are not as flexible as in the case of micelles and liquid crystals, i.e., the atoms which form the cavity wall are rigid and will not give way to the expanding reaction cavity.

A striking difference in product distribution (E/C ratio) between zeolites is seen in the case of **1c–f** (Table III). On the basis of the results in Table III, in broad terms, the zeolites can be classified into two sets: One set of zeolites (ZSM-5, ZSM-11, ZSM-34, and offretite) has channel dimensions less than 6.5 Å and yields only the elimination product, acetophenone. The other set of zeolites (X, Y, L, Ω-5, and M-5) has channel or cage dimensions larger than 7 Å and yields both the elimination and cyclization products, with the E/C ratios differing slightly between the zeolites. We propose that this large difference arises from the difference in the size of the reaction cavity for the two sets of zeolites. We choose for discussion Na X and ZSM-5 as representatives for the large and small reaction cavity zeolites, respectively. The fact that type II products are obtained in ZSM-5 indicates that the smaller reaction cavity (~5.5-Å diameter) hinders but does not completely prevent the attainment of the required geometry for hydrogen abstraction by the triplet ketone. As pointed out earlier, the rate of hydrogen abstraction (τ_t^{-1}) is directly related to the mole fraction of the favorable isomers present in the equilibrium.[16,17] From the diffuse reflectance laser flash photolysis lifetime studies it is clear that the rate of intramolecular hydrogen abstraction in ZSM-5 is reduced considerably with respect to that in Na X (Table II). This suggests that intramolecular hydrogen abstraction within ZSM-5 channels occurs from a very high energy, briefly populated conformation.

How and why does the primary 1,4-diradical undergo a preferential elimination process within the channels of ZSM-5? Our attempts to directly monitor the 1,4-diradical derived from valerophenone have not been successful, indicating that the biradical is too short-lived to be detectable in the presence of relatively long-lived triplets. We ascribe the preferential occurrence of the elimination process not to an enhanced cleavage but to a decreased cyclization yield due to restrictions imposed by the zeolite interior. One can visualize that the skew diradical can give elimination products either directly or via the transoid diradical. This process will compete with fast intramolecular back hydrogen transfer yielding the starting ketone. Such an intramolecular hydrogen return will lower the efficiency of, but will not inhibit, type II product formation. As illustrated in Scheme IV, the formation of cisoid diradical from the skew geometry will result in substantial motion of either the aryl or the alkyl substituents. Permanent displacement of these groups from their original positions can not be accommodated by the small reaction cavity provided by the narrow channels (~5.5-Å diameter). Similarly, direct conversion of the skew diradical to the cyclobutanol will not be tolerated by the medium. These conclusions are supported by the fact that the cyclobutanols from aryl alkyl ketones are too bulky to fit within the narrow channels. In fact, our attempts to include the cyclobutanol from octanophenone, prepared by solution photolysis, into ZSM-5, ZSM-11, and ZSM-8 were not successful. Thus, we conclude that cyclization from the skew diradical (either directly or via the cisoid diradical) cannot occur within the channels of ZSM zeolites. If this is the case, can elimination occur directly from the skew diradical? It would probably have to occur from a geometry which does not involve complete overlap of the singly occupied p orbitals with the central bond being broken since a complete overlap requires large motions of the aryl and alkyl substituents as described above. Cleavage, if it occurs, probably occurs from a compromise conformation involving small nonbonded interactions and only partial orbital overlap.[25,27]

Scheme IV

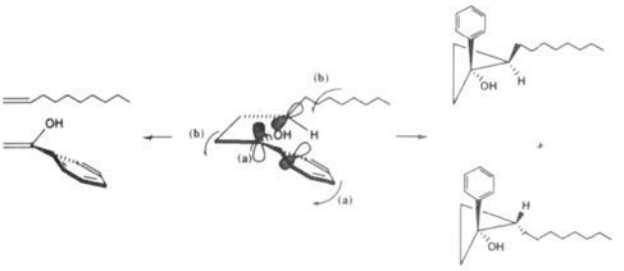

The alternative pathway available to the skew diradical is the conversion to the transoid form which can only cleave. The linear transoid diradical, once formed, will easily fit into the narrow channels of ZSM. It has been suggested by Weiss et al.[29] that conversion from the skew to the transoid form of the diradical can be achieved without much change in the molecular volume by the wiggly motions of the alkyl chain. Such a process has been invoked by Weiss to explain the results in liquid crystalline medium and is termed "crankshaft" motion.[30] Such motions do not require large ancillary motion of the groups attached to the 1,4 positions of the type II 1,4-diradical. A similar motion termed "hula twist" was proposed by Liu et al.[31] for specific geometric isomerization of polyenes. This process converts transoid to cisoid forms in addition to geometric isomerization of one of the double bonds. Such processes are attractive since they require a small molecular volume and involve fairly small displacement of the substituent groups. While these may not be the preferred motions in solution, in a confined medium such as a zeolite channel they may be the only ones by which the intermediates can decay. Once the skew diradical converts to the transoid geometry by either of the above

(27) Wagner, P. J.; Kelso, P. A.; Kemppainen, A. E.; McGrath, J. M.; Schott, H. N.; Zepp, R. G. *J. Am. Chem. Soc.* **1972**, *94*, 7506.
(28) Cohen, M. D. *Angew. Chem., Int. Ed. Engl.* **1975**, *14*, 386. Venkatesan, K.; Ramamurthy, V. In *Photochemistry in Organized and Constrained Media*; Ramamurthy, V., Ed.; VCH: New York, 1991; p 133.
(29) Hrovat, D. A.; Liu, J. H.; Turro, N. J.; Weiss, R. G. *J. Am. Chem. Soc.* **1984**, *106*, 7033.
(30) Zimmerman, R. G.; Liu, J. H.; Weiss, R. G. *J. Am. Chem. Soc.* **1986**, *108*, 5264.
(31) Liu, R. S. H.; Browne, D. T. *Acc. Chem. Res.* **1986**, *19*, 42. Liu, R. S. H.; Asato, A. *Proc. Natl. Acad. Sci. U.S.A.* **1985**, *82*, 259.

Table VI. Dependence of the Physical Parameters of M Y Zeolites on the Cation

cation (M^+)	ionic radius of the cation (Å)[a]	electrostatic field (V/Å) within the cage[a]	electrostatic potential (e/r)[a]	spin–orbit coupling[b] of the cation	vacant space[c] within the supercage (Å^3)	
					Y zeolite	X zeolite
Li	0.6	2.1	1.67	–	834	873
Na	0.95	1.3	1.05	27	827	852
K	1.33	1.0	0.75	87	807	800
Rb	1.48	0.8	0.67	360	796	770
Cs	1.69	0.6	0.59	840	781	732

[a] Ward, R. J. *J. Catal.* **1968**, *10*, 34. [b] McGlynn, S. P.; Azumi, T.; Knoshita, M. *Molecular Spectroscopy of the Triplet State*; Prentice Hall: Englewood Cliffs, NJ, 1969. [c] Calculations of polyhedral volumes were performed using a modification of the POLYVOL program (Swanson, D.; Peterson, R. C. *Can. Mineral.* **1980**, *18* (2), 153. Swanson, D. K.; Peterson, R. C. POLYVOL Program Documentation, Virginia Polytechnic Institute: Blacksburg, VA) assuming the radius of the TO_2 unit to be 2.08 Å (equivalent to that of quartz).

motions (or via any other motions available to it), it can only decay to elimination products.

The above model would predict that as the size of the reaction cavity increases or as the aryl or alkyl substituent size decreases, the contribution of the cisoid diradical to the product distribution should increase. It is indeed comforting to note that this is the case. Zeolites M-5 and Ω-5, which have channel structures with channel sizes larger (>7 Å) than that present in ZSM-5 (~5.5 Å), give both cyclobutanol and acetophenone. Even higher yields of cyclobutanol are obtained within X and Y zeolites which have a cage diameter of ~12 Å. Thus, there is a clear trend in the yield of cyclobutanol: X, Y > M-5, Ω5 > ZSM-5, ZSM-34. It is important to note that the size of the cavity or channel wherein the reaction occurs also increases in that order. Consistent with this model, when the alkyl group is small, as in the case of butyrophenone (**1a**) and valerophenone (**1b**), small amounts of cyclization products are indeed obtained in pentasil zeolites (Table III). These are completely absent for ketones with larger alkyl groups. A preliminary study[32] with a large number of dialkyl ketones such as 2-alkanones, 3-alkanones, and 4-alkanones has also shown that these systems yield both the elimination and the cyclization products via the type II process within ZSM-5, ZSM-8, and ZSM-11 zeolites. In these cases, the large phenyl substituent is replaced with the smaller alkyl group.

In the above analyses of the results, we have not made any statements concerning the rate of interconversion between the diradical conformers (skew, cisoid, and transoid). The triplet diradical lifetime in solution is long enough to allow conformational equilibrium,[33] but it is not clear whether the same applies in zeolite channels or cavities.[34] We plan to pursue this question further.

Consequences of the Modification of the Reaction Cavity. A. Cation Effect. As the cation present within the supercage is varied, several properties of the cage change: electric field (micropolarity) within the cage, the extent of the spin–orbit coupling mechanism available for singlet–triplet interconversion, and the cage free volume (Table VI). The external spin–orbit coupling mechanism is not expected to play an important role in the photoreaction of aryl alkyl ketones.[35] As we discussed earlier, an interaction between the cation and the carbonyl group has been indicated by IR, UV absorption, and TGA studies. Examination of Table IV reveals that the effect of the cation on the product distribution is significant in X but not in Y zeolites. While cation binding is expected to influence the behavior of the ketone in both X and Y zeolites, the absence of cation effects on the product distribution in Y zeolites suggests that interaction between the cation and the carbonyl chromophore is not playing a significant role in the decay, via elimination and cyclization processes, of the type II 1,4-diradical. Therefore, we attribute the cation effects to changes in the cage free volume upon cation exchange.

A look at Table VI reveals that upon cation exchange a much larger decrease in cage free volume occurs in X than in Y zeolites. This is due to the absence or reduced number of type III ions in Y zeolites (Figure 1). Among the various zeolites listed in Table VI, Rb X and Cs X have the lowest cage free volume. It is important to note that the *trans*- to *cis*-cyclobutanol ratio is significantly higher only in these two zeolites (Rb X and Cs X). We attribute the enhancement of the *trans*-cyclobutanol in cavities of smaller sizes (<770 Å^3) to the differences in size and shape of the *cis*- and *trans*-cyclobutanols. *cis*-Cyclobutanol with the aryl and alkyl groups on the same side is expected to be bulky and spherical in shape while the *trans*-cyclobutanol is expected to be long and cylindrical in shape. The diradical precursors of these *trans*- and *cis*-cyclobutanols will also have closely related shapes. While the *trans*-cyclobutanol and its precursor diradical can fit between two cages, the *cis*-cyclobutanol and its precursor diradical will have to fit within a single cage. However, when the cage free volume is not large enough to accommodate the *cis*-cyclobutanol and its precursor diradical, it is obvious that the formation of *trans*-cyclobutanol will be favored. It is interesting to note that the *trans*- to *cis*-cyclobutanol ratio is constant up to a free volume of 780 Å^3, independent of the cation or the nature of the zeolite (X or Y). This confirms that it is indeed the cage free volume which is responsible for the change in the *trans*- to *cis*-cyclobutanol yield.

As pointed out above, there is certainly an interaction between the cation and the ketone within the supercages of X and Y zeolites. While this interaction influences the primary step of the reaction, namely, hydrogen abstraction (as indicated by changes in triplet lifetime), it has no effect on the E/C and *trans*- to *cis*-cyclobutanol ratio.

B. Role of Intracavity Solvent Hexane. From Table IV it is clear that the E/C ratio decreases (i.e., cyclization is enhanced) when dry zeolite is replaced with a zeolite–hexane slurry. Such a reduction in the E/C ratio also agrees well with the reaction cavity model discussed above. The enhanced cyclization yields must result from larger contributions from the cisoid diradical. Why is the cisoid contribution enhanced in supercages filled with solvent molecules? As discussed above, in X and Y zeolites both transoid and cisoid conformers of the 1,4-diradical participate in the formation of elimination and cyclization products. Transformation of the skew diradical (the primary 1,4-diradical) to the transoid and the cisoid forms will be controlled by the size of the reaction cavity wherein it is present. Of these two processes the conversion to the transoid form (requires 180° rotation of the central σ-bond and 90° rotation of the C–C bond carrying the aryl and OH groups) will require a larger displacement of the solvent molecule present inside the cage. Note that this is not the process by which the initial biradical is proposed to be converted to the transoid form in the more restricted space within the ZSM-5 channels; in this case, a high-energy pathway was proposed as the motions required for the low-energy pathway are not tolerated by the narrow channels. On the other hand, conversion to the cisoid form requires only a 90° rotation of the C–C bond carrying the aryl and OH groups and, thus, a correspondingly reduced displacement of the solvent. It is obvious on this basis that solvent-filled cages will favor the formation of the cisoid rather than the transoid diradical from the primary skew diradical. Such a preference will be reflected as an increase in the cyclization process. The results observed in Na X, K X, Na Y, and K Y slurries with hexane are indeed consistent with this expectation. In order to appreciate the results, it is important to realize that

(32) Ramamuthy, V.; Sanderson, D. R. *Tetrahedron Lett.*, in press.
(33) Scaiano, J. C. *Tetrahedron* **1982**, *38*, 819.
(34) He, Z.; Weiss, R. G. *J. Am. Chem. Soc.* **1990**, *112*, 5535.
(35) Lower, S. K.; El-Sayed, M. *Chem. Rev.* **1966**, *66*, 199.

hexane present within the supercages of zeolites does not have the same properties as in solution. Although in a zeolite–solvent slurry the solvent present in the supercages will be in equilibrium with the bulk solvent, it ("intracrystalline solvent") is expected to have microproperties different from those of the bulk solvent. The heat of adsorption and the activation energy for self-diffusion of hexane in Na X have been measured to be ~18 kcal mol^{-1} and ~5 kcal mol^{-1}, respectively.[36] The self-diffusion coefficient for hexane within Na X has been measured to be at least 2 orders of magnitude lower than in the bulk liquid.[37] As a result of the reduced diffusivities of the "intracrystalline solvent", and due to the reduced space within the supercage, the mobility of guests present within solvent-filled supercages is expected to be reduced even further than that in solvent-free supercages. Therefore, hexane molecules present in supercages present a high barrier for mobility of guest molecules. However, they are not as rigid as the zeolite walls, which do not permit any shape changes; hexane molecules present within zeolites can respond to shape changes although not to the same extent as in isotropic solution. Thus, the presence of hexane enables one to fine-tune the properties of the zeolite cavity.

Summary

The results of the present study of a large number of aryl alkyl ketones within a number of zeolites have revealed that the conformational distribution of the ground-state ketone as well as that of the diradical intermediate is influenced by the zeolite medium. Our results have not clearly established whether there is an equilibrium between the conformer of the ketone excited state and whether the diradical conformers are equilibrated before they decay to the final products. Further work is needed to clarify this aspect.

A model that has emerged from this study is that in order for the medium to exert the maximum influence on a chemical process, the "reaction cavity" or the volume within which the reactants are confined has to be small. A "reaction cavity" that is too large will permit the molecule to undergo motions similar to those in solution, and the selectivity will be low. On the other hand, providing no free space around the reactant, i.e., too small a "reaction cavity", may completely prevent the reaction, which, of course, is not to our benefit. This could occur in a crystalline medium. The reaction cavity must be small enough and soft enough to respond to the shape changes that occur along the reaction coordinate, but at the same time it must provide sufficient restriction to the reactive intermediates to obtain selectivity. The above concept can encompass other media such as micelles, liquid crystals, inclusion complexes, and crystals as well as zeolites. The selectivity of the type II reaction has been investigated in a variety of these media. For example, in micelles there is little selectivity, consistent with the large and soft micellar structure which can easily accommodate shape changes of the guest molecules.[38] A higher selectivity has been obtained in liquid crystalline media which are less rigid than crystals but still provide a barrier to shape changes.[39] Poor selectivity has been obtained for type II reaction of aryl alkyl ketones in Dainin's compound.[40] This result is easily rationalized on the basis of the above model, since the reaction cavity in this host is relatively large (11 × ~6 Å). When the cavity size is decreased as in the case of cyclodextrin (~5.6 × 7.8 Å)[41] and urea (~5.3 Å)[42] inclusion complexes, a higher selectivity is indeed observed. These examples indicate that the reaction cavity concept can satisfactorily explain results for the type II reaction in a variety of confined media and serves as a useful basis for the development of a more general model.

Zeolites have been demonstrated to be useful media for photophysical and photochemical studies of included molecules. These supports are commercially available, and their properties can be modified to a certain extent by cation-exchange techniques. Despite their opaque and powdery appearance, there is no difficulty in carrying out photochemistry of molecules included within zeolites. Furthermore, a number of recent improvements in techniques such as solid-state NMR and diffuse reflectance flash photolysis should improve our understanding of the behavior of included molecules. One of the advantages of zeolites over other heterogeneous systems such as micelles, liquid crystals, and monolayers is the fact that the medium cannot be perturbed by the guest molecules and thus provides a rigid reaction cavity. However, it is presently difficult to predict with any certainty the location and distribution of guest molecules within the zeolites. Zeolites have been extensively used for a variety of industrial processes, but we are only now starting to address the question of how the zeolite lattice controls the reactivity and selectivity of included species.

Experimental Section

Materials. All ketones used in this study were purchased from Aldrich and were purified by either vacuum distillation or recrystallization.

Zeolites 13X (Na X) and LZ-Y52 (Na Y) were obtained from Linde. The cation of interest was exchanged into these powders by contacting the material with the appropriate nitrate solution at 90 °C. For each gram of zeolite, 10 mL of a 10% nitrate solution was used. This was repeated a number of times. The samples were then thoroughly washed with water and dried. Exchange loadings were typically between 37 and 84%. Exchange levels for individual zeolites were as follows: Li X, 46%; K X, 64%; Rb X, 49%; Cs X, 37%; Li Y, 64%; K Y, 84%; Rb Y, 68%; Cs Y, 62%. Prior to use, these samples were heated in a furnace at 500 °C in air for about 10 h. Activated zeolites were used immediately.

Samples of Na TPA-ZSM-5 with Si/Al varying from 20 to 550 were prepared by slight modification of Rollman and Volyocsik's procedure.[43] Samples were calcined in flowing air at 60 °C/h to 550 °C and then held at 550 °C for 10 h to give Na ZSM-5. The samples were then exchanged by conventional methods to give Li ZSM-5, K ZSM-5, Rb ZSM-5 and Cs ZSM-5. All samples were subjected to elemental analysis. These samples were stored under ambient conditions.

Zeolites were activated as follows. In general, ca. 250 mg of zeolite was placed in a silica crucible and heated at 500 °C for about 12 h. The freshly activated zeolites were rapidly cooled in air to ca. 50 °C and added to solutions of the ketones of interest. Activated zeolites were used immediately after activation. In general, we have found that the time required for these activated zeolites to readsorb water to their full capacity is about 10 h under our laboratory conditions, and of course this varies with the zeolites. The rehydration is easily monitored by keeping the activated zeolites on the pan of an analytical balance and watching the weight change.

Thermogravimetric analyses were carried out on a Du Pont Model 951 thermogravimetric analyzer. IR spectra were recorded on a Nicolet Model 60-SX IR spectrometer.

Preparation of Zeolite Complexes. A. Dry Solid Zeolites. Known amounts of phenyl alkyl ketones and the activated zeolites were stirred together in 20 mL of hexane (in the case of X, Y, M-5, and Ω-5 zeolites) or trimethylpentane (all other zeolites) for about 10 h. In a typical preparation, 250 mg of the zeolite and 5 mg of the ketone were taken in 20 mL of the solvent. White powder collected by filtration of the solvent was washed with dry hexane several times and dried under nitrogen. Samples were taken in Pyrex cells fitted with Teflon stopcocks, degassed thoroughly (10^{-5} mm), and sealed. These samples were generally dry and contained less than 1% of water.

For irradiation at different loading levels complexes were prepared by the above procedure in which the Na X amount was kept constant at 250

(36) Tsitsishvili, G. V.; Andronikashvili, T. G. In *Molecular Sieve Zeolites*; Flanigen, E. M., Sand, L. B., Eds.; American Chemical Society: Washington, DC, 1971; pp 217–228. Avgul, N. N.; Bezus, A. G.; Dzhigit, O. M. In *Molecular Sieve Zeolites*; Flanigen, E. M., Sand, L. B., Eds.; American Chemical Society: Washington, DC, 1971; pp 184–192. Ruthven, D. M.; Doetsch, I. H. *AIChE J.* **1976**, *22*, 882.

(37) Karger, J.; Pfeifer, H.; Rauscher, M.; Walter, A. *J. Chem. Soc., Faraday Trans. I* **1980**, *76*, 717. Karger, J.; Pfeifer, H.; Walther, P.; Dyer, A.; Williams, C. D. *Zeolites* **1988**, *8*, 251.

(38) Turro, N. J.; Liu, K. C.; Cow, M. F. *Photochem. Photobiol.* **1977**, *26*, 413.

(39) For a review: Weiss, R. G. In *Photochemistry in Organiced and Constrained Media*; Ramamurthy, V., Ed.; VCH: New York, 1991; p 603.

(40) Goswami, P. C.; de Mayo, P.; Ramnath, N.; Bernard, G.; Omkaram, N.; Scheffer, J. R.; Wong, Y. F. *Can. J. Chem.* **1985**, *63*, 2719.

(41) Dasaratha Reddy, G.; Jayasree, B.; Ramamurthy, V. *J. Org. Chem.* **1987**, *52*, 3107.

(42) Casal, H. L.; de Mayo, P.; Miranda, J. F.; Scaiano, J. C. *J. Am. Chem. Soc.* **1983**, *105*, 5155.

(43) Rollman, L. S.; Volyocsik, E. K. *Inorganic Synthesis*; Wiley: New York, 1983; pp 61–68.

mg and the ketone amount was varied between 0.5 and 20 mg.

B. Zeolite-Hexane Slurry. Known amounts of guest ketones and the activated zeolites were stirred together in 5 mL of hexane for about 2 h. In a typical preparation, 200 mg of the zeolite and 5 mg of ketone were taken in 5 mL of the solvent. At the end of 2 h, the hexane layer was analyzed by GC for the presence of the ketone in the hexane portion. In no case did we find any guest in the hexane layer, indicating that all the initial ketone had been adsorbed into the zeolite.

Photophysical Studies. Diffuse reflectance spectra of the zeolite solid samples were measured in 2-mm-path-length quartz cells using a Varian 2400 spectrometer equipped with either an integrating sphere (Varian) or a "Praying Mantis" all-reflective light collection system (Harrick Scientific), in both cases using barium sulfate (Kodak, white reflectance standard) as the reference. Sample packing densities were not determined nor were they specifically controlled. Spectra were recorded between 220 and 500 nm. For comparison, spectra of the empty zeolites were also recorded. Data were recorded digitally, and appropriate background corrections were carried out using the computer program SpectraCalc (Galactic Industries).

Emission spectra were recorded at room temperature and at 77 K in Supracil quartz EPR tubes under degassed conditions with a Spex Fluorolog 212 spectrofluorimeter.

The experimental setup for diffuse reflectance laser flash photolysis measurements has been described elsewhere.[44] For these experiments, the fourth harmonic (266 nm, 10-ns pulses, ≤25 mJ/pulse) from a Lumonics HY-750 Nd:YAG laser was used for sample excitation. The samples were contained in 3 × 7 mm^2 quartz cuvettes and were deaerated by purging for at least 30 min with oxygen-free nitrogen. During the laser experiments the sample was either moved or shaken to ensure that a fresh sample surface was used for each laser shot.

Photolysis Studies. A. Dry Samples. Samples containing 125 mg of the complex were degassed in Pyrex cells and irradiated with 450-W mercury lamps. Irradiation cells were rotated periodically to provide uniform exposure. Generally about 15% conversion was obtained in about 2 h of irradiation. After photolysis, products were extracted by stirring the samples in ether (20 mL) for about 6 h. In some cases the zeolite was dissolved with concentrated HCl and extracted with ether. Control experiments established that the products are stable to the acid extraction conditions.

B. Zeolite-Hexane Slurry. A guest-zeolite-solvent slurry in a Pyrex test tube was purged with helium (making sure no evaporation of hexane occurred) for about 10 min and sealed. The above slurry was magnetically stirred and irradiated with 450-W mercury lamps with Pyrex filters for about 30 min. The hexane (or pentane) solvent was decanted and analyzed by GC. Neither starting reactants nor products were found in the supernatant solvent. Products and reactants were extracted from the zeolites by stirring them with diethyl ether (10 mL) for about 10 h. The ether extract was analyzed by GC as above.

Products from both dry zeolites and hexane slurries were analyzed by GC (Hewlett Packard Model 5890, SE-30 capillary column) and peaks were integrated with a Hewlett Packard integrator Model 3393A. The temperature of the analysis was between 80 and 250 °C depending on the ketone. The flame-ionization detector was not calibrated for differences in detector response to the various products and starting ketone. The elution order was as follows: solvent, acetophenone, type II olefin, *cis*-cyclobutanol, *trans*-cyclobutanol, and starting ketone. All peaks were identified by coinjection with authentic samples. *cis*- and *trans*-cyclobutanols were obtained by large-scale solution irradiation (2 × 50 mg/25 mL of benzene) and isolation by silica gel flash chromatography. These were characterized by comparison of their IR, NMR, and mass spectra with the literature reports.[25,30,41] It is to be noted that the *trans*-cyclobutanol elutes before the cis isomer during the silica gel flash chromatography.

Acknowledgment. It is a pleasure to thank D. Sanderson and P. Hollins for able technical assistance and Professors R. G. Weiss and P. Wagner for valuable discussions.

Registry No. 1a, 495-40-9; **1b**, 1009-14-9; **1c**, 1674-37-9; **1d**, 1674-38-0; **1e**, 4497-05-6; **1f**, 6786-36-3; AcPh, 98-86-2; Li, 7439-93-2; Na, 7440-23-5; K, 7440-09-7; Rb, 7440-17-7; Cs, 7440-46-2; $CH_3(CH_2)_4C-H_3$, 110-54-3; 1-phenylcyclobutanol, 935-64-8; 2-methyl-1-phenylcyclobutanol, 82245-43-0; *cis*-2-butyl-1-phenylcyclobutanol, 95605-57-5; *trans*-2-butyl-1-phenylcyclobutanol, 95605-56-4; *cis*-2-octyl-1-phenylcyclobutanol, 126583-83-3; *trans*-2-octyl-1-phenylcyclobutanol, 126583-82-2; *cis*-2-decyl-1-phenylcyclobutanol, 126583-85-5; *trans*-2-decyl-1-phenylcyclobutanol, 126583-84-4; *cis*-1-phenyl-2-tetradecylcyclobutanol, 126583-87-7; *trans*-1-phenyl-2-tetradecylcyclobutanol, 126583-86-6.

(44) Kazanis, S.; Azarani, A.; Johnston, L. J. *J. Am. Chem. Soc.* **1991**, *95*, 4430.

Heavy-Atom-Induced Phosphorescence of Aromatics and Olefins Included within Zeolites

V. Ramamurthy,* J. V Caspar, D. F. Eaton, Erica W. Kuo, and D. R. Corbin

Contribution No. 6068 from Central Research and Development, Experimental Station, The Du Pont Company, Wilmington, Delaware 19880-0328. *Received December 2, 1991*

Abstract: Photophysical properties of naphthalene and other aromatic guest molecules included in X-type faujasite zeolites (M^+ X, M = Li, Na, K, Rb, Cs, Tl) have been investigated. As expected for an external heavy atom perturbed excited state, both singlet and triplet excited state lifetimes and emission efficiencies depend upon the identity and accessibility of the cation present within the zeolite supercage. The large magnitude of the external-heavy-atom perturbation is not unique to the X-type faujasites; similar effects for organic guests included in Y-type faujasites, in pentasils (ZSM-5 and ZSM-11), and in other zeolites (mordenite, β, L, and Ω) have been demonstrated. The power of the heavy-atom-cation effect in zeolites has been demonstrated by recording phosphorescence data from several olefins whose phosphorescence data has not been recorded previously. The heavy atom cation induced phosphorescence technique has been utilized to understand basic features of interaction between the zeolite and guest aromatic molecules.

Introduction

Studies utilizing a number of organized assemblies and surfaces to orient molecules have paved the way to an intriguing number of possibilities by which photochemical and photophysical properties of molecules can be modified.[1] In this context, the internal surfaces of zeolites have attracted recent attention.[2] Zeolites may be regarded as open structures of silica in which aluminum has been substituted into a number of the tetrahedral sites.[3] The

(1) Kalyanasundaram, K. *Photochemistry in Microheterogeneous Systems*; Academic Press: New York, 1987. Ramamurthy, V., Ed. *Photochemistry in Organized and Constrained Media*; VCH: New York, 1991.

(2) Turro, N. J. *Pure Appl. Chem.* **1986**, *58*, 1219. Turro, N. J. In *Molecular Dynamics in Restricted Geometries*; Klafter, J., Drake, J. M., Eds.; John Wiley: New York, 1989; p 387. Turro, N. J.; Garcia-Garibay, M. In *Photochemistry in Organized and Constrained Media*; Ramamurthy, V., Ed.; VCH: New York, 1991; p 1. Ramamurthy, V. In *Photochemistry in Organized and Constrained Media*; Ramamurthy, V., Ed.; VCH: New York, 1991; p 429. Kelly, G. K.; Willsher, C. J.; Wilkinson, F.; Netto-Ferreira, J. C.; Olea, A.; Weir, D.; Johnston, L.; Scaiano, J. C. *Can. J. Chem.* **1990**, *68*, 812 and other papers in the series. Sankaraman, S.; Yoon, K. B.; Kochi, J. K. *J. Am. Chem. Soc.* **1991**, *113*, 1419 and other papers in the series.

0002-7863/92/1514-3882$03.00/0